

The Φ -factory DA Φ NE as a source of infrared radiation: An estimate of source size and brilliance

A. Nucara and P. Calvani

Università La Sapienza, Dipartimento di Fisica, P.le A. Moro 1, 00100 Roma, Italy

A. Marcelli

I.N.F.N.-Laboratori Nazionali di Frascati, Casella Postale 13, 00044 Frascati, Italy

M. Sánchez del Río

European Synchrotron Radiation Facility, B.P. 220, 38043 Grenoble-Cedex 9, France

(Presented on 19 July 1994)

The actual source area of a bending magnet emitting in the infrared range, has been calculated for the double annular Φ -factory for nice experiments (DA Φ NE) under construction at Frascati. "Geometrical" broadening has been included. The actual brilliance ratio defined as the ratio between the brilliance of a synchrotron source and that of a blackbody, has been also evaluated for DA Φ NE and compared with the Brookhaven NSLS source. © 1995 American Institute of Physics.

I. THE ACTUAL SOURCE AREA

An estimate of the source size is the first step to obtain the actual brilliance ratio (ABR), or the gain of a storage ring over a blackbody. The brilliance is defined as the flux dF emitted by the actual source area (ASA) in the small solid angle $d\theta d\psi$,

$$B = \left(\frac{dF}{d\theta d\psi (2\pi \Sigma_x \Sigma_y)} \right) \text{ photons/s/cm}^2/\text{rad}^2. \quad (1)$$

In Eq. (1), F is the flux of photons emitted by the particles along their trajectory, $d\theta$ and $d\psi$ are the horizontal and vertical emission angles, x and y the horizontal and vertical coordinates. Here, Σ_x and Σ_y are the rms values of the horizontal and vertical dimensions, and $2\pi \Sigma_x \Sigma_y$ is the area which approximates an extended source. A general expression for the ASA has to take into account any possible contribution: geometrical broadening, physical effects, and the ring parameters associated with the dynamics of the electron beam. By generalizing a well-known formula of Ref. 1, we can write

$$\begin{aligned} \text{ASA} &= 2\pi \Sigma_x \Sigma_y \\ &= 2\pi \sqrt{\sigma_x^2 + \sigma_r^2 + (\sigma_x^{\text{geo}})^2} \sqrt{\sigma_y^2 + \sigma_r^2 + (\sigma_y^{\text{geo}})^2}, \end{aligned} \quad (2)$$

where

$$\sigma_x = \sqrt{\sigma_{0x}^2 + \sigma_{Mx}^2} = \sqrt{\epsilon_x \beta_x + (\eta_x \sigma_\epsilon)^2}, \quad (3)$$

$$\sigma_y = \sqrt{\sigma_{0y}^2 + \sigma_{My}^2} = \sqrt{\epsilon_y \beta_y \frac{\epsilon_y^2 + \epsilon_y \gamma_y \sigma_r^2}{\sigma_\psi^2}}, \quad (4)$$

σ_r is the diffraction-limited source size, while σ_x^{geo} and σ_y^{geo} are "geometrical" terms. The latter have been here in-

roduced to represent the broadening of the source due to the electron path over a finite spatial length of the bending magnet (BM). In Eqs. (3) and (4), the electron beam dimensions σ_{0i} ($i=x,y$) are added to the broadenings σ_{Mi} due to the BM dispersion. As usual, σ_ψ is the opening angle of the radiation, η_x is the dispersion function in the x direction at the bending magnet (BM) source point ϵ_y is the vertical emittance, σ_ϵ the relative rms energy spread in the anomalous bunch lengthening regime, and γ_y is the Twiss parameter in the vertical plane.^{2,3} In the IR range, σ_ψ becomes very large leading to a vertical size comparable with, or greater than, the horizontal dimension.

By using the above equations and the parameter values reported in Refs. 4 and 5, σ_x and σ_y have been calculated for bending magnet sources of both DA Φ NE and NSLS. The results are reported in Table I. The vertical contribution σ_{My} from the optical functions of the machine is calculated for $\lambda=50 \mu\text{m}$ and results to be much smaller than σ_{0y} . However, it may become comparable with σ_{0y} at higher wavelengths.

The effect of diffraction has then been taken into account in the following way. From standard optics, a source point emitting at the wavelength λ under an angle $\sigma_\psi(\lambda)$ has a minimum dimension given by

$$\sigma_r(\lambda) = \frac{\lambda}{4\pi\sigma_\psi(\lambda)}. \quad (5)$$

In the present case

$$\sigma_\psi(\lambda) = 0.816 \left(\frac{\lambda}{\lambda_c} \right)^{0.354} \frac{10^{-3}}{E(\text{GeV})} (\text{rad}). \quad (6)$$

In the above relation, the exponent of (λ/λ_c) has been derived in the limit $\lambda/\lambda_c \gg 1$, obviously valid in the IR range.⁶

TABLE I. Estimated values of synchrotron source size for $\lambda=50 \mu\text{m}$. Data are taken from Refs. 5 and 4 for NSLS and DA Φ NE, respectively.

BM	E (GeV)	ϵ_x (10^{-6} cm rad)	ϵ_y (10^{-6} cm rad)	σ_{Mx} (cm)	σ_{My} (10^{-5} cm)	σ_x (cm)	σ_y (cm)
NSLS	0.745	13.8	0.4	0.045	1.4	0.058	0.0197
DA Φ NE	0.51	100	1	0.0198	3.2	0.217	0.031

However, different expressions for such energy range are reported in the literature, which exhibit quite similar behaviors.^{7,8}

The diffraction-limited size given by Eq. (5) increases if one considers the extended source as a surface placed in the middle of the curved electron trajectory. At the first optical element the source is seen under a horizontal angle θ and a vertical angle $\sigma_\psi(\lambda)$, so that the radiation is collected with a solid angle $\Omega = \theta\sigma_\psi$. This effect contributes to the ASA by

$$\sigma_{LD}^2 = \frac{\lambda^2}{(4\pi)^2 \Omega}. \quad (7)$$

II. THE GEOMETRICAL BROADENINGS σ_x^{geo} and σ_y^{geo}

The terms σ_x^{geo} and σ_y^{geo} in Eq. (2) are usually negligible in the x-ray and soft x-ray ranges, where small angles are collected by the optics. This is not true in the IR range, where the radiation has a large natural divergence. As the collecting angle θ of a BM increases, a SR source becomes an arc of length $2\theta\rho$, where ρ is the radius of the BM, whose projection on the x - y plane gives a horizontal broadening Δ . The intersection of the x - y plane with the trajectory is also assumed to be the virtual location of the extended source. In the IR range, and for large collecting angles ($\theta > 10$ mrad), Δ cannot be neglected. A first attempt to estimate the "geometrical" size of the source was made by Williams.⁸ He started from the expression

$$\Delta = \rho(1 - \cos \theta/2). \quad (8)$$

Here, Δ is greater than the rms value σ_x^{geo} in Eq. (2). The latter quantity has been estimated in a separate paper. One finds⁹

$$(\sigma_x^{\text{geo}})^2 = \langle x^2 \rangle - \langle x \rangle^2 = \frac{3}{2} \rho^2 + \rho^2 \frac{\sin \theta}{2\theta} - \rho^2 4 \frac{\sin \theta/2}{\theta} - \rho^2 \left(1 - \frac{2}{\theta} \sin \frac{\theta}{2} \right)^2. \quad (9)$$

Similarly, one obtains for the vertical geometrical broadening:⁹

TABLE II. Input ray-tracing parameters.

	E (GeV)	λ_c (Å)	σ_x (mm)	σ_y (mm)	θ (mrad)	ρ (cm)
DAΦNE	0.51	59.6	2.17	0.313	50	140
NLS	0.745	25.5	0.58	0.197	50	191

$$(\sigma_y^{\text{geo}})^2 = \langle y^2 \rangle = \frac{\rho^2 t g^2 (\sigma_\psi/2)}{2\theta} \times \left[\sin^2 \left(\frac{\theta}{2} \right) \tan \left(\frac{\theta}{2} \right) - \theta + 2 \sin \left(\frac{\theta}{2} \right) \right]. \quad (10)$$

III. COMPARISON WITH RAY-TRACING SIMULATION AND DISCUSSION

The terms σ_x^{geo} and σ_y^{geo} , once calculated by Eqs. (9) and (10), respectively, can be compared for different IR wavelengths with the size of the source generated by computer simulation. We have simulated the DAΦNE and the NLS bending magnet sources by using the ray-tracing code SHADOW,¹⁰ and by starting from the ring parameters⁴ reported in Table II. The resulting σ_x^{sim} and σ_y^{sim} are reported in Table III for both rings. In Table III, they can also be compared with σ_x^{geo} and σ_y^{geo} , as obtained from Eqs. (9) and (10) and from the calculated average displacement $\langle x \rangle$ reported in the same table. For the y direction, values at four different λ 's are reported. One should notice that σ_x^{sim} includes both σ_x and the geometrical contribution, while the diffraction term σ_r is excluded. The same holds for σ_y^{sim} .

When looking at the data reported in Table III, one sees that the NLS horizontal size is mainly determined by σ_x . The σ_x^{geo} contribution obtained by ray-tracing simulation (not reported in the table) is just 0.201 mm, very similar to the one calculated by Eq. (9) and listed in Table III. For the NLS source, ray tracing results give $\langle x \rangle = 0.2$ mm, in excellent agreement with the value calculated in Table III (0.199 mm).

In the case of DAΦNE, the geometrical broadening obtained by ray-tracing simulation (not reported in the table) is $\sigma_x^{\text{geo}} = 0.37$ mm. This value is greater than the calculated one. Indeed, it is affected by a considerable uncertainty due to the large horizontal dimension of the electron beam, which masks any other effect. In the case of NLS, the beam size and the geometrical horizontal broadening are of the same order of magnitude. On the other hand, the ray-tracing values

TABLE III. Ray-tracing of the source size (σ_i^{sim}), geometrical contributions (σ_i^{geo}) and diffraction terms of the source size at different λ . Simulation has been performed with a collecting angle of 50 mrad. $\langle x \rangle_{\text{th}}$ is the horizontal displacement of the beam calculated as in Ref. 9.

	$\langle x \rangle$ (mm)	σ_x^{geo} (mm)	σ_y^{geo}				σ_r (mm)				σ_x^{sim} (mm)	σ_y^{sim} (mm)			
			$\lambda=10$	$\lambda=100$	$\lambda=1000$	$\lambda=5000$	$\lambda=10$	$\lambda=100$	$\lambda=1000$	$\lambda=5000$		$\lambda=10$	$\lambda=100$	$\lambda=1000$	$\lambda=5000$
NLS	0.199	0.177	0.198	0.45	1.02	1.81	0.039	0.172	0.761	2.15	0.601	0.198	0.37	0.732	1.23
DAΦNE	0.146	0.130	0.158	0.357	0.808	1.433	0.036	0.159	0.703	1.99	2.202	0.34	0.462	0.739	1.089

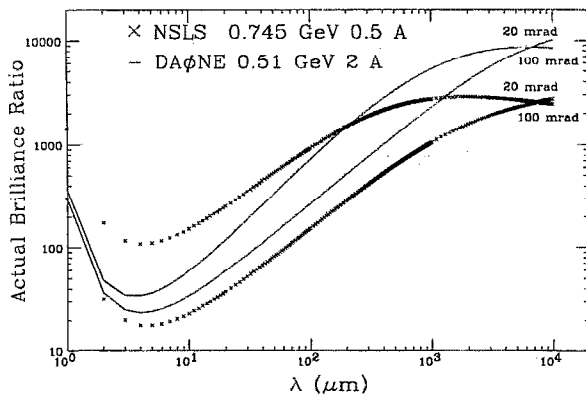


FIG. 1. The ABR function for a DAΦNE BM source (continuous lines) and for a NSLS BM source, as calculated for horizontal collecting angles θ of 20 and 100 mrad.

for the vertical dimension are in good agreement with those calculated by Eq. (10).

In addition to the large geometrical contributions, further effects associated with the interference of light may modify the spectral angular distribution of SR in the far IR range.¹¹ The function $D(\lambda) = 2\pi \sum_x \sum_y \Omega + \lambda^2$ for small wavelengths ($\lambda < 1 \mu\text{m}$) is almost independent of λ and exhibits a simple power law. At wavelengths of the same order of the ASA ($\lambda \sim 1 \text{ mm}$) the diffraction limit introduces significant deviations from the power law. At very large λ (cm range) it becomes the most important contribution to the actual source area.

A comparison between the infrared radiation extracted from DAΦNE and that from a conventional source can be finally obtained by calculating the actual brilliance ratio (ABR), namely, the ratio between the brilliance of the synchrotron source (B_{SR}) and the brilliance of a blackbody (B_{BB}) at 2000 K. The former quantity will be given by

$$B_{\text{SR}} = \left. \frac{d^2 F}{d\theta d\psi} \right|_{\psi=0} / \text{ASA}(\text{cm}^2) \quad \text{photons}/0.1\% \text{BW}/\text{s}/\text{cm}^2/\text{rad}^2, \quad (11)$$

where

$$\frac{d^2 F}{d\theta d\psi} = 1.327 \times 10^{19} E^2(\text{GeV}) I(\text{A}) \left(\frac{\lambda_c}{\lambda} \right)^2 K_{2/3}^2 \left(\frac{\lambda_c}{2\lambda} \right) \quad (12)$$

is the flux of photons in the solid angle for a bandwidth $\Delta\nu = 0.001\nu$. By using the criterion reported in Ref. 12, we can evaluate the modified Bessel function in the limit $\lambda_c/2\lambda = 0.002$. For DAΦNE $\lambda_c = 59.6 \text{ \AA}$, so that this relation is verified for frequencies higher than $1.5 \mu\text{m}$. On the other hand,

$$B_{\text{BB}}(\lambda, T) = \frac{2}{\lambda^3} \frac{0.001c}{(e^{\beta h c/\lambda} - 1)} \quad \text{photons}/0.1\% \text{BW}/\text{s}/\text{cm}^2/\text{str}. \quad (13)$$

The ABR is calculated by means of the ASA values here obtained. The results are shown in Fig. 1 for both DAΦNE and the NSLS. Figure 1 shows the advantage of the SR sources on the blackbody at all wavelengths, for collecting

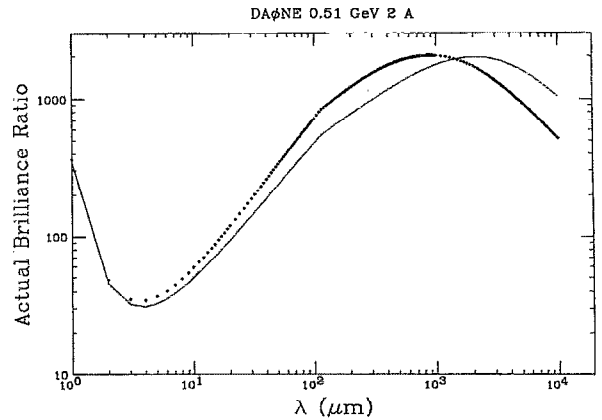


FIG. 2. The “actual” ABR function for DAΦNE with an exit port at 120 cm from the BM source, which limits the vertical collecting angle to 50 mrad. The dotted curve corresponds to a 20 mrad horizontal collecting angle, the solid one to 50 mrad.

angles of 20 and 100 mrad. For larger angles (i.e., 100 mrad) the gain is reduced for both rings due to a larger source area. When comparing the two sources with each other, one sees that the NSLS BM is more brilliant at short λ , due to the smaller value of its source size.

In the case of DAΦNE, for a front end with a slit which limits the vertical collecting angle, the ABR is appreciably reduced only at very large wavelengths, as shown in Fig. 2.

In conclusion, we have determined the ASA, including the geometrical contributions, and the ABR for the new beamline which is under project for the high-current Φ -factory DAΦNE. The brilliance in the far infrared is expected to be higher than for a blackbody by two orders of magnitude or more. Our results are consistent with ray-tracing computer simulation, and will be very useful in the design of the infrared SR DAΦNE beamline optics.¹³ Comparisons with the performances of a BM of the NSLS in the infrared, have also been reported.

ACKNOWLEDGMENTS

The authors wish to thank R. Cöisson and P. Roy for useful discussions.

- ¹ S. L. Hulbert and J. M. Weber, Nucl. Instrum. Methods A **319**, 25 (1992).
- ² “Synchrotron Radiation and Free Lasers,” CERN Accelerator School, Chester, 1989, CERN 90-03.
- ³ S. Krinsky, M. Perlman, and R. E. Watson, in *Handbook on Synchrotron Radiation*, edited by E. E. Koch (North Holland, Amsterdam, 1983), Vol. 1, Chap. 2.
- ⁴ M. E. Biagini, C. Biscari, S. Guiducci, J. Lu, M. R. Masullo, and G. Vignola, DAΦNE Technical Note L-9, 1993.
- ⁵ J. Murphy, Synchrotron Light Source Data Book, BNL 42335 IR, 1990.
- ⁶ X-Ray Data Booklet, Center for x-ray optics, PUB 490 Lawrence Berkeley Laboratory, University of California.
- ⁷ W. D. Duncan and G. P. Williams, Appl. Opt. **22**, 2914 (1983).
- ⁸ G. P. Williams, Nucl. Instrum. Methods **195**, 383 (1982).
- ⁹ A. Nucara, P. Calvani, A. Marcelli, and M. Sanchez del Rio, LNF Internal Report No. 94/053(IR), 1994.
- ¹⁰ C. Welnak, G.-J. Chen, and F. Cerrina, Nucl. Instrum. Methods A **347**, 344 (1994).
- ¹¹ R. Cöisson, J. Phys. **45**, L89 (1984).
- ¹² V. O. Kostroun, Nucl. Instrum. Methods **172**, 371 (1980).
- ¹³ E. Burattini, G. Cappuccio, A. Marcelli, P. Calvani, A. Nucara, and M. Sanchez del Rio, Nucl. Instrum. Methods A **347**, 308 (1994).